INSTITUTE OF PHYSICS PUBLISHING JOURNAL OF PHYSICS D: APPLIED PHYSICS

J. Phys. D: Appl. Phys. **36** (2003) 818–822 PII: S0022-3727(03)57144-3

Carbon-nanotubes on graphite: alignment of lattice structure

C Rettig[1], M Bödecker and H Hövel[2]

University of Dortmund, Experimentelle Physik I, 44221 Dortmund, Germany
E-mail: hoevel@physik.uni-dortmund.de

Received 4 December 2002
Published 19 March 2003
Online at stacks.iop.org/JPhysD/36/818

Abstract
We study the alignment of the lattice structure of single walled carbon-nanotubes (SWNT) produced on a highly oriented pyrolytic graphite (HOPG) surface using controlled growth in ultrahigh vacuum (UHV). With scanning tunnelling microscopy (STM) at low temperature ($T = 77$ K) the HOPG and the SWNT were imaged in UHV simultaneously with atomic resolution. The lattice structure of the SWNT was compared to the HOPG. For this purpose we present a technique for evaluating the mutual orientation which uses the measured lattice vectors of the HOPG surface as a reference for distortion and drift effects in the STM image. The quantitative evaluation showed an alignment of the SWNT lattice structure to the structure of the substrate.

1. Introduction

The detailed mechanism of carbon-nanotube growth is still a topic of current research. The controlled growth of single walled carbon-nanotubes (SWNT) with a given diameter and structure would be essential for many applications, in particular electronics.

Recently, several publications have described the first steps in the manufacture of nanotubes with control of the tube characteristics, e.g. [1, 2]. For SWNT grown with controlled production in ultrahigh vacuum (UHV) using the method recently described in [3] we have observed an alignment of the SWNT lattice with the lattice of the highly oriented pyrolytic graphite (HOPG) substrate, which was measured simultaneously with the SWNT.

Here we show the detailed analysis of this alignment using scanning tunnelling microscopy (STM) images measured at $T = 77$ K. The analysis utilizes the HOPG surface as a reference. It includes the drift- and calibration-effects of the piezo-crystal and the expansion of the STM image perpendicular to the SWNT axis due to the imaging of a curved surface. The observed alignment of the SWNT and the HOPG lattice may show a way to control the tube structure, if, additionally, the orientation of the tube axis can be selected.

[1] Present address: European Synchroton Facility, ESRF, BP 220, 38043 Grenoble Cedex, France.
[2] Author to whom correspondence should be addressed.

2. Experimental

For the production of the nanotube sample we used a new method which is described in detail in [3], but here we give a short summary. The surface of HOPG was nanostructured with 1 monolayer (ML) deep circular pits [4], which were made in two steps. First we sputtered the surface with argon to induce defects, then we oxidized the defects in an Ar/O_2-atmosphere to 1 ML deep pits with approximately 10 nm diameter. Subsequently metal clusters were produced by the thermal evaporation of metal atoms on this prestructured surface, which condensed in the nanopits [4]. After the cluster-growth, the sample was heated and carbon was deposited on the surface. It is well known that carbon deposition on a surface covered with transition metal particles leads to nanotube growth [1]. We used different parameters for the cluster-size and material, the amount of carbon deposited on the surface and the temperature during the deposition [3]. The best results for the SWNT growth were found for Co-clusters and a 3 nm effective film thickness of carbon deposited at 900°C. Without metal-clusters we did not observe a nanotube growth.

This sample was measured with STM [5] at room temperature and at $T = 77$ K. At room temperature the STM-tip was not stable and changed its shape. In general this led to a large width of the tip, which did not allow atomic resolution of the substrates and the nanotubes. Another problem at room temperature was the creep of the piezo-crystal. Starting with an overview image of our sample,

we had to zoom inside on a position which showed a SWNT. After repositioning of the tip the creep led to a large drift of the piezo-crystal [6, 7], which moved the tip outside the interesting part of the sample.

To take stable images of the surfaces with atomic resolution on the substrate and the nanotubes, we measured at low temperature ($T = 77$ K). At this temperature the state of the tip was more stable and drift-effects were also minimized. The STM imaging of nanotubes with atomic resolution needs an especially well defined tip shape, which required an extensive additional preparation of the electrochemically etched tungsten tips. First, we had to reduce the tip-width and remove multiple tips by a controlled collision of the tip with the Co-clusters, using a high scan speed. After overview images showed well separated clusters and nanotubes with flat HOPG areas in-between (typical tunnelling condition $U = 1.2$ V, $I = 0.1$ nA), we tried to achieve atomic resolution on large parts of the flat HOPG. For this purpose the tip was prepared by stopping the scan and applying a high voltage $U = 2$–10 V with a tunnelling current $I = 0.1$ nA. With these two steps, we were able to prepare the tip several times to get atomic resolution on the substrate and the nanotubes. For the small detailed images with atomic resolution of the nanotubes (typical tunnelling condition $U = 1.0$ V, $I = 0.3$ nA), we oriented the fast scan direction of the STM parallel to the nanotube axis. In this way we avoided collisions of the tip with the nanotubes.

We were able to reach atomic resolution on different parts of the nanotubes and simultaneously on the HOPG substrate. One of the imaged nanotubes is shown in figure 1(*a*), showing different parts of the nanotube. Figure 1(*b*) shows a junction with a measured height difference of about 0.2 nm, an angled connection is shown in figure 1(*c*) and the cap at the end of the nanotube is shown in figure 1(*d*). In figure 1(*b*) the small extra hillock at the junction can be explained due to the pentagonal and heptagonal defects incorporated in the junctions [8]. Figure 1(*d*) shows atomic resolution also at the end of the tube, but we were not able to collect enough information from the caps to make a comparison with the expected fullerene-like structures.

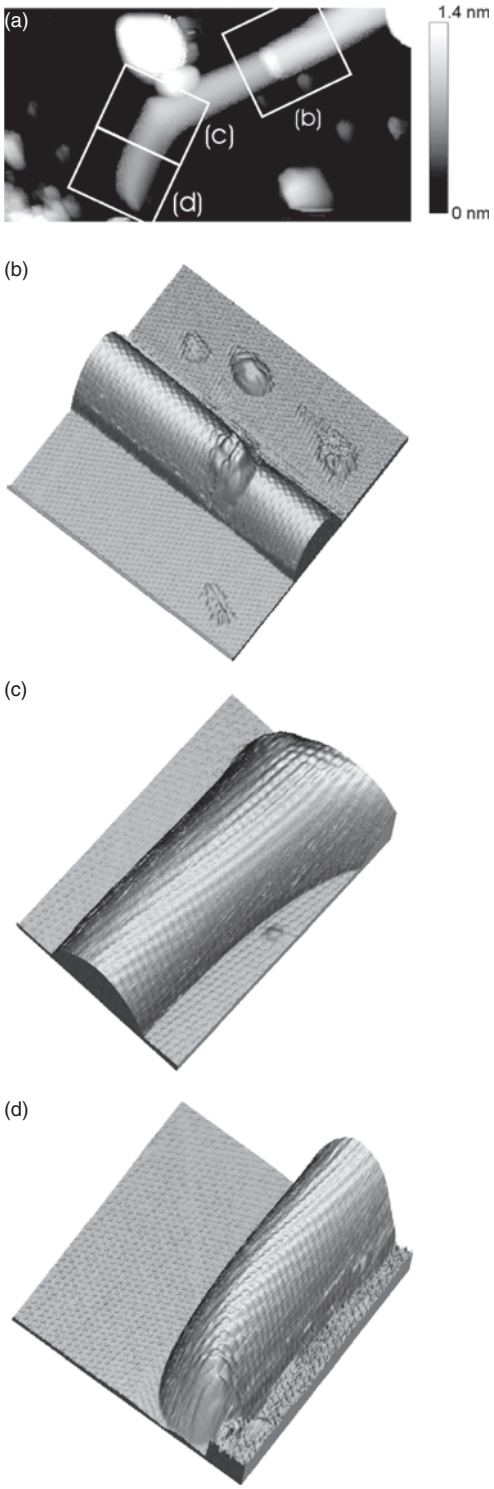

Figure 1. STM images of a SWNT measured at $T = 77$ K. (*a*) Overview image (50×25 nm^2). The boxes mark the parts shown in (*b*) (14×14 nm^2), (*c*) (11×8 nm^2) and (*d*) (11×11 nm^2).

3. Analysis of the atomically resolved STM images

In figure 2 the lattice structure of the SWNT and the HOPG is shown. One can see a small distortion of the lattice structure of the HOPG with different periodicities in different directions. To explain the distortion, we use a model which contains drift effects of the piezo-crystal. We take the lattice vectors for the HOPG ($\vec{b}_1$ und $\vec{b}_3$) and SWNT ($\tilde{\vec{b}}_1$ und $\tilde{\vec{b}}_3$) from periodic grids fitted to the images. To describe the distortion- and calibration-effects of the lattice vectors, we define the two ideal graphene lattice vectors $\vec{e}_1 = (\cos(30^\circ), \sin(30^\circ)) = (e_{1x}, e_{1y})$ and $\vec{e}_3 = (0, -1) = (e_{3x}, e_{3y})$ with $|\vec{e}_1| = |\vec{e}_3| \equiv 1$, $\sphericalangle(\vec{e}_1, \vec{e}_3) = 120^\circ$ and multiply these vectors with a matrix, called a 'map matrix', with the components A_{ij}. This product has to be equal to the measured lattice vectors of the HOPG

$$\begin{pmatrix} A_{xx} & A_{xy} \\ A_{yx} & A_{yy} \end{pmatrix} \cdot \begin{pmatrix} e_{1x} & e_{3x} \\ e_{1y} & e_{3y} \end{pmatrix} = \begin{pmatrix} b_{1x} & b_{3x} \\ b_{1y} & b_{3y} \end{pmatrix}. \qquad (1)$$

The x-direction for the measured vectors $\vec{b}_1$ und $\vec{b}_3$ is parallel to the fast scan direction (which corresponds to the SWNT axis for the images with atomic resolution).

The same procedure was used for the measured lattice vectors of the nanotubes. The nanotube map matrix is different from the HOPG map matrix. Using equation (1), one is able to evaluate the map matrices of HOPG or of the SWNT,

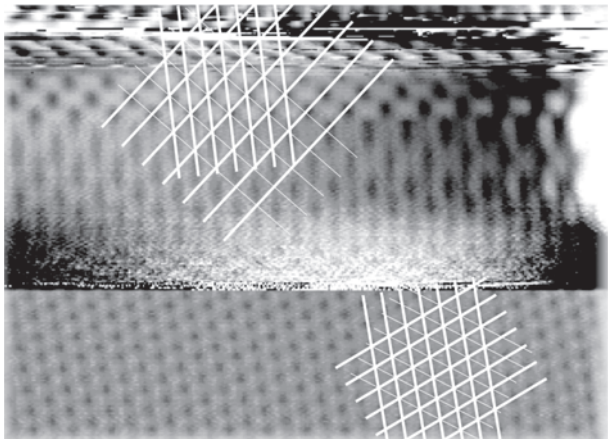

Figure 2. STM image ($6 \times 8\,\mathrm{nm}^2$) of part (*b*) from the SWNT of figure 1 at $T = 77$ K. Top left: triangular lattice (white solid lines) fitted to the SWNT. Bottom right: lattice fitted to HOPG. The mean height was subtracted for each horizontal scan line in order to stretch the colour scaling for atomic resolution.

respectively

$$\begin{pmatrix} A_{xx} & A_{xy} \\ A_{yx} & A_{yy} \end{pmatrix} = \begin{pmatrix} b_{1x} & b_{3x} \\ b_{1y} & b_{3y} \end{pmatrix} \cdot \begin{pmatrix} e_{1x} & e_{3x} \\ e_{1y} & e_{3y} \end{pmatrix}^{-1}. \tag{2}$$

Up to now we did not make any assumptions for the map matrices. Considering the definition of $(\vec{e}_1, \vec{e}_3)$ and $(\vec{b}_1, \vec{b}_3)$ the map matrix includes a rotation matrix

$$\begin{pmatrix} \cos(\beta) & \sin(\beta) \\ -\sin(\beta) & \cos(\beta) \end{pmatrix}. \tag{3}$$

The angle β describes the angle between the fixed vectors of the ideal graphene and the measured vectors of the graphene. In addition the map matrices have to contain drift- and calibration-effects of the piezo-crystal, here described with the components d_{ij}

$$\begin{pmatrix} d_{xx} & d_{xy} \\ d_{yx} & d_{yy} \end{pmatrix}. \tag{4}$$

One is not able to calculate all variables d_{ij} and β, because the equations are under-determined.

Figure 3 shows the distortion and calibration effects of each component of the drift- and calibration-matrix. The drift of the piezo-crystal is a very slow effect in comparison to the timescale of the fast scan direction of the STM [6, 7]. In our case the fast scan speed is parallel to the x-direction and the slow scan direction is parallel to the y-direction with a factor 400 slower than the fast scan speed. Therefore the y-position of one fast scan line is constant in good approximation. The x-position of different fast scan lines is shifted. So one has to take account of the distortion in the xy- but not in the yx-component. With these assumptions the equation for the HOPG is given by

$$\begin{pmatrix} d_{xx} & d_{xy} \\ 0 & d_{yy} \end{pmatrix} \cdot \begin{pmatrix} \cos(\beta) & \sin(\beta) \\ -\sin(\beta) & \cos(\beta) \end{pmatrix} = \begin{pmatrix} A_{xx} & A_{xy} \\ A_{yx} & A_{yy} \end{pmatrix}. \tag{5}$$

The corresponding equation for the SWNT is

$$\begin{pmatrix} \tilde{d}_{xx} & \tilde{d}_{xy} \\ 0 & \tilde{d}_{yy} \end{pmatrix} \cdot \begin{pmatrix} \cos(\alpha) & \sin(\alpha) \\ -\sin(\alpha) & \cos(\alpha) \end{pmatrix} = \begin{pmatrix} \tilde{A}_{xx} & \tilde{A}_{xy} \\ \tilde{A}_{yx} & \tilde{A}_{yy} \end{pmatrix} \tag{6}$$

with the rotation angle α and all other variables with a tilde relating to the nanotubes.

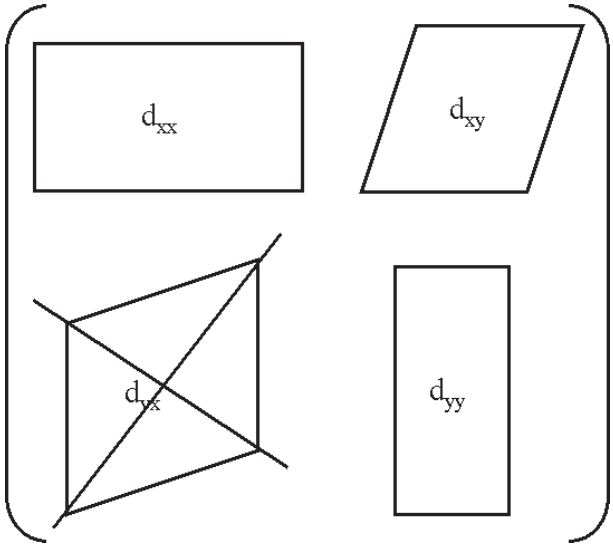

Figure 3. Schematic drawing showing the effects of each component of the distortion matrix on the lattice vectors. Compared to the y-direction, the scan speed in the x-direction is a factor 400 higher. This is the reason for neglecting the component d_{yx}.

To explain the different values of the drift- and calibration-matrix components, we have to take account of the detailed geometry concerning the image process for the nanotubes, as described in [8]. In our case, the slow scan direction is perpendicular to the nanotube axis. The distance d between the SWNT and the tip is assumed to be constant. With this, the tip moves on a circular path of radius $r + d$ around the axis of the nanotube with radius r. For the image near the top of the nanotube this results in an expansion in the y-direction perpendicular to the nanotube axis, by the factor $z = 1 + d/r$. First we calculate the drift- and calibration-matrix and the angle β of the HOPG. We take the drift- and calibration-matrix of the HOPG to determine the distortion effects for the measured image. These effects are assumed to be constant for the whole image, i.e. to be the same on the HOPG surfaces and on the SWNT. The additional y-distortion is inserted between the drift- and calibration-matrix of the HOPG and the rotation matrix of the SWNT. This product has to be equal to the calculated map matrix of the SWNT.

$$\underbrace{\overbrace{\begin{pmatrix} d_{xx} & d_{xy} \\ 0 & d_{yy} \end{pmatrix}}^{\text{HOPG}} \cdot \begin{pmatrix} 1 & 0 \\ 0 & z \end{pmatrix} \cdot \begin{pmatrix} \cos(\alpha) & \sin(\alpha) \\ -\sin(\alpha) & \cos(\alpha) \end{pmatrix}}_{E} = \begin{pmatrix} \tilde{A}_{xx} & \tilde{A}_{xy} \\ \tilde{A}_{yx} & \tilde{A}_{yy} \end{pmatrix}. \tag{7}$$

The matrix E is given by the two parameters z and α

$$\begin{pmatrix} E_{xx}(z,\alpha) & E_{xy}(z,\alpha) \\ E_{yx}(z,\alpha) & E_{yy}(z,\alpha) \end{pmatrix} = \begin{pmatrix} \tilde{A}_{xx} & \tilde{A}_{xy} \\ \tilde{A}_{yx} & \tilde{A}_{yy} \end{pmatrix}. \tag{8}$$

To determine the best values of the two parameters, we sum up the square differences of the components from both matrices. The inverse of this sum is maximal for the best fit of z and α

$$S = \big((E_{xx} - \tilde{A}_{xx})^2 + (E_{xy} - \tilde{A}_{xy})^2 + (E_{yx} - \tilde{A}_{yx})^2 + (E_{yy} - \tilde{A}_{yy})^2\big)^{-1} \equiv \max. \tag{9}$$

A graph of this function with the data out of figure 2 is shown in figure 4. To determine the values for α and z we take a profile crossing the maximum parallel to the z-axis or α-axis, respectively. These profiles can be fitted in good approximation by Lorentzians. We take the values of the parameters α and z as given by the maxima of the Lorentzians. The half width at the half maximum is used as an approximation of the error.

4. Results and discussion

We studied three tubes with seven different parts in total. We were able to measure 14 atomically resolved images of six different parts. By using the presented model for the evaluation of the images, we get the graph shown in figure 5. This graph shows the rotation angle β of the HOPG and α of the SWNT. The line shows the equation $\alpha = \beta$. One can see that the data points are located close to the line within the error bars.

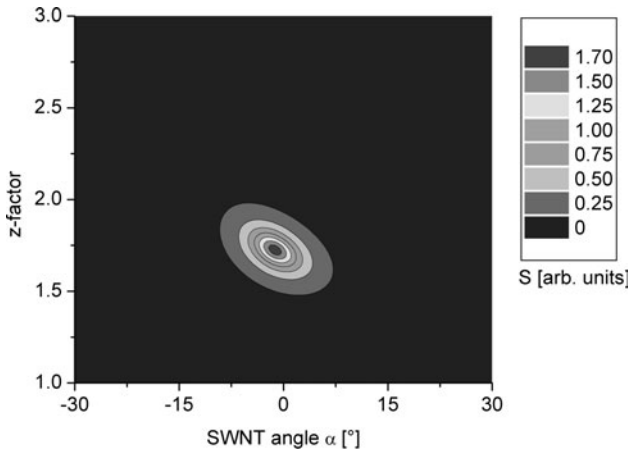

Figure 4. Plot of the function (8) of the SWNT shown in figure 2 with the fit parameters α and z. To determine the best values of these parameters we take profiles through the maximum. The FWHM of these profiles is taken as an estimation of the error.

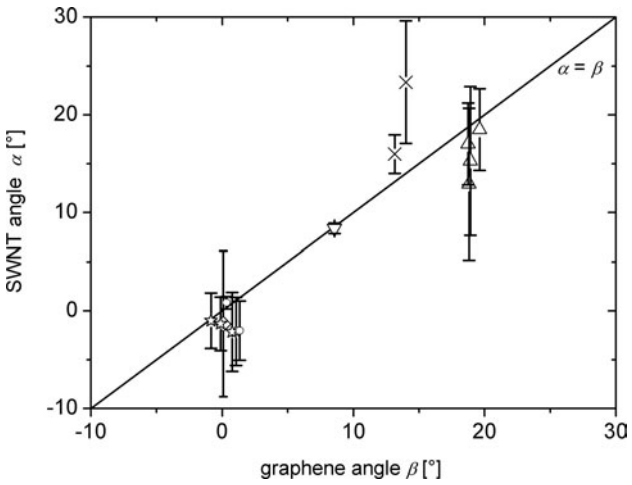

Figure 5. Graph showing the alignment of the lattice of the SWNT and the HOPG. Symbols are related to the six different SWNT parts. Different results for one symbol are due to different atomically resolved SWNT images. The solid line shows the equation $\alpha = \beta$, which indicates an alignment of the lattice structure of the SWNT and the HOPG substrate.

Only two points (shown as $\times$) show a significant deviation. The errors of these data points are relatively large, because we could only use a short line of atoms for the lattice fit of the SWNT. With our fitting procedure an inaccurate fit of the lattice results in large error bars. Accordingly, one of the two data points with the smaller error bar is closer to the line.

Even if the number of data points is not very large, the correlation of α and β in figure 5 shows a significant alignment of the lattices of the SWNT and the HOPG. This is not restricted to a small part of the sample because the data points in figure 5 were measured for three macroscopically different positions.

As the SWNT axes are parallel to the fast scan direction, i.e. parallel to the x-direction in our model, we can deduce the chiral angles of the SWNT from their lattice rotation angle. The chiral vector, which defines the chiral angle, is perpendicular to the SWNT axis. With our definition of $\vec{e}_1$ and $\vec{e}_3$ the lattice rotation angle corresponds to the usual definition of the chiral angle, i.e. $\alpha = 0$ for a zig-zag-tube. All angles β of HOPG are positive or have only very small negative angles near 0°. Our model allows negative angles. With more data also larger negative angles ($-30° < \beta < 0°$) should occur.

The special alignment of the lattice of the SWNT grown on the HOPG surface maximizes the interaction energy. The binding of SWNT on graphite is similar to the interaction of two graphite planes. This means that the interaction between SWNT and graphite is weak and is van der Waals in origin. An interaction energy of 2 eV per nm tube length was calculated for similar SWNT diameters [9]. In our case one has to consider the interaction energy difference of aligned and misaligned SWNT relating to the substrate. This energy difference is much smaller than 2 eV per nm tube length. Calculated interaction energies as a function of the nanotube orientation [9], together with corresponding experiments [10], show sharp energy minima, which lead to a locking into the aligned lattice structures. The energy gain for these directions is about 10 meV per nm tube length. To discuss if these interactions are the reason for the experimentally observed lattice alignment, we consider the thermal vibrations of freestanding SWNT grown out of a fixed metal particle, which are dominated by the 0th harmonic mode [11]. With a tube length of 25 nm and a diameter of 1.5 nm one gets a vibration amplitude of $u_0 \approx 0.1$ nm at room temperature, which corresponds to an energy of $(1/2)c_0u_0^2 = k_BT$. Higher harmonics and longitudinal modes have much smaller amplitudes. At $T = 900$°C the amplitudes will be a factor 2 larger but nevertheless only the 0th harmonic will have an amplitude of the order of the HOPG lattice constant. With this it is possible that despite of the thermal vibrations the energy barrier of $25\,\text{nm} \times 10\,\text{meV nm}^{-1} \approx 250$ meV for the aligned structure will influence the growth process if one compares it with $k_BT \approx 100$ meV at 900°C.

For comparison we also made STM measurements for SWNT, which were produced by the method of Smalley and co-workers [12]. These SWNT were deposited out of a Toluol suspension on the HOPG surface. The STM images of these samples showed no single SWNT but bundles of SWNT (cf figure 6). We were not able to achieve atomic resolution for these samples, because the bundles were displaced by the influence of the tip—in contrast to the more stable measurements discussed above. This is an additional indication of the energy barrier for a tube displacement caused by the alignment in the case of the SWNT grown on HOPG.

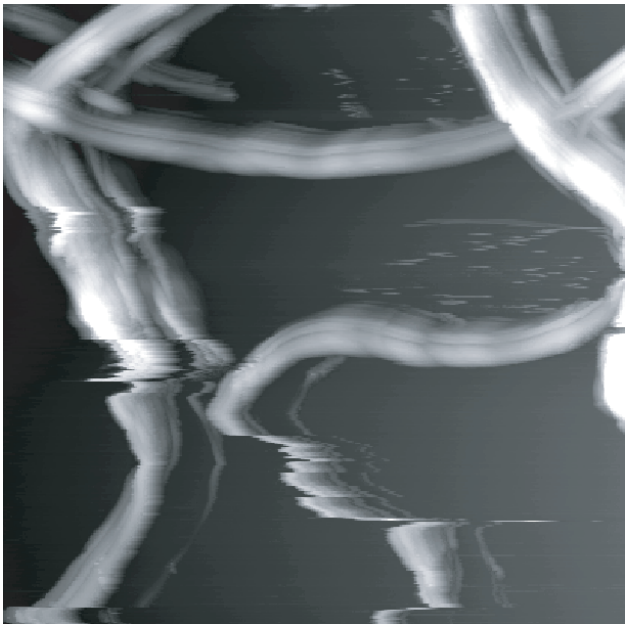

Figure 6. STM image ($500 \times 500\,\mathrm{nm}^2$, $T = 300\,\mathrm{K}$). The image shows bundles of SWNT with a height of $\approx$10 nm produced in the gas phase [12] and deposited from a Toluene suspension on HOPG. One can see the movement of the bundles induced by the tip movement, which made atomic resolution on these samples impossible.

We mention however measurements for short SWNT deposited out of solution on HOPG, which showed a preferential orientation of the nanotubes. This maximized the interaction energy and indicated a very high purity of the production process [13].

5. Conclusions

We presented the results of a STM study of catalytically grown SWNT on HOPG, where atomic resolution was achieved by using low temperature ($T = 77\,\mathrm{K}$). This temperature minimized the drift effects of the STM and stabilized the STM tip. Under these conditions we were able to measure the SWNT and the substrate HOPG simultaneously with atomic resolution.

We developed a model to determine the relative orientation of the HOPG and the SWNT, which utilizes the measured HOPG surface as reference. A simple matrix formalism, which includes the drift- and calibration-effects of the piezo-crystal and the expansion of the STM image perpendicular to the SWNT axis due to the imaging of curved surface, was used to measure the lattice orientations of the HOPG and the SWNT. In addition this model contains an estimation of the error for the rotation angle of each SWNT. In this way we were able to compare quantitatively the lattice orientations of the HOPG and the SWNT. We showed that the lattice structure of the HOPG is aligned to the lattice structure of the SWNT. This result agrees with theoretical calculations [9] and the measurements [10] of the interaction energy of SWNT and HOPG. Finally we can say that our new production process which uses the depositon of Co-clusters on prestructured HOPG surfaces as catalytic centres within the subsequent deposition of carbon, leads to an aligned growth of SWNT on the substrate.

If we would be able to produce SWNT with a fixed direction for the tube axis on a graphite single crystal, we would obtain with our process in addition a fixed chiral angle. On HOPG this would be valid for an area of several $\mu\mathrm{m}^2$, i.e. on a single crystallite of the polymorphic crystal. This would offer the possibility to determine and to control the electronic and geometric properties of the produced SWNT.

Acknowledgments

The authors would like to acknowledge support by the Deutsche Forschungsgemeinschaft (Ho-1597/3-3).

References

[1] Dresselhaus M S, Dresselhaus G and Avouris Ph (ed) 2001 Carbon nanotubes: synthesis, structure, properties and applications *Topics in Applied Physics* vol 80 (Berlin: Springer)
[2] Kong J, Soh H T, Cassell A M, Quate C F and Dai H 1998 *Nature* **395** 878
[3] Hövel H, Bödecker M, Grimm B and Rettig C 2002 *J. Appl. Phys.* **92** 771
[4] Hövel H, Becker Th, Bettac A, Reihl B, Tschudy M and Willliams E J 1997 *J. Appl. Phys.* **81** 154
[5] Hövel H, Becker T, Funnemann D, Grimm B, Quitmann C and Reihl B 1998 *J. Electron Spectrosc. Rel. Phenom.* **88–91** 1015
[6] McKeith N E, Smith R W and Whiteford J R 1975 *J. Phys. E: Sci Instrum.* **9** 15
[7] Basedow R W and Cocks T D 1980 *J. Phys. E: Sci. Instrum.* **13** 15
[8] Meunier V and Lambin Ph 1998 *Phys. Rev. Lett.* **81** 5588
[9] Budlum A and Jing Ping Lu 1990 *Phys. Rev. Lett.* **83** 5050
[10] Falvo M R, Steele J, Taylor II R M and Superfine R 2000 *Phys. Rev.* B **62** 10665
[11] Krishnan A, Dujardin E, Ebbesen T W, Yianilos P N and Treacy M M 1998 *Phys. Rev.* B **58** 14013
[12] Guo T, Nikolaev P, Thess A, Colbert D T and Smalley R E 1995 *Chem. Phys. Lett.* **243** 49
[13] Andrew J L *et al* 1998 *Science* **280** 1253